

Received 13 January 2023, accepted 31 January 2023, date of publication 6 February 2023, date of current version 14 February 2023.

Digital Object Identifier 10.1109/ACCESS.2023.3243162

## SURVEY

# Application of Artificial Intelligence Methods in Carotid Artery Segmentation: A Review

YU WANG<sup>1</sup> AND YUDONG YAO<sup>2</sup>, (Fellow, IEEE)

<sup>1</sup>College of Medicine and Biological Information Engineering, Northeastern University, Shenyang 110016, China

<sup>2</sup>Department of Electrical and Computer Engineering, Stevens Institute of Technology, Hoboken, NJ 07030, USA

Corresponding author: Yudong Yao (Yu-Dong.Yao@stevens.edu)

**ABSTRACT** The carotid artery is one of the most important blood vessels that supply blood to the brain. If thrombus occurs, it may cause cerebral ischemic stroke and endanger life. Carotid intima-media thickness and stability of carotid plaque are essential indicators for predicting stroke, which can be measured through medical image segmentation. Therefore, automatic and accurate carotid artery image segmentation and measurement of carotid intima-media thickness and the area and volume of carotid plaque are of great significance for stroke risk prediction and treatment. However, due to the complex shape of the carotid artery and the characteristics of carotid artery imaging, the traditional methods (such as threshold methods, region growth methods) can not segment the carotid artery very well. In recent years, researchers have taken artificial intelligence (traditional machine learning and deep learning) as a critical research method for carotid artery segmentation and extensive research has been performed with satisfactory results. In this paper, we present a comprehensive review of carotid artery segmentation using artificial intelligence methods. We first briefly introduce medical image processing methods and artificial intelligence methods. And then, review and summarize the application of artificial intelligence segmentation methods in carotid artery segmentation (including carotid lumen, media-adventitia, lumen-intima, and plaques). Finally, the challenges of current artificial intelligence methods in carotid artery segmentation are analyzed.

**INDEX TERMS** Carotid artery segmentation, plaque segmentation, medical image processing, machine learning, deep learning.

## I. INTRODUCTION

The carotid artery is one of the most important blood vessels that supply blood to the brain, providing more than 80% of the brain's blood [1]. A patient suffering from carotid artery disease may experience reduced blood flow to the brain and, in turn, their blood circulation system can be affected. In severe cases, it can cause cerebral infarction, stroke and other diseases, endangering life and safety. The primary reason of carotid artery disease is carotid artery stenosis caused by intimal plaque deposition and medial calcification. Carotid artery disease diagnosis mainly depends on imaging for examination. Commonly used carotid artery imaging methods include magnetic resonance imaging (MRI), computed tomography angiography (CTA),

and ultrasound imaging (US). These three imaging methods have their advantages and disadvantages, and each has its unique application scenario. Among them, MR has better clarity and clinical sensitivity, which can directly reflect the carotid artery condition, but the cost is the highest. Compared with MR, CTA has a slightly lower image resolution and is accompanied by ionizing radiation, but the cost is lower than that of MR. As the least-cost imaging method, US has the advantages of real-time and no ionizing radiation, but the US image has the problems of low contrast and strong noise.

With the analysis of carotid artery images, we can make risk prediction and treatment decisions for carotid disease through the following two methods, carotid stenosis assessment [2] and carotid plaque analysis [3]. The degree of carotid stenosis can be evaluated by calculating the carotid lumen diameter ratio to adventitia diameter in carotid images [4]. Carotid plaque analysis mainly refers to plaque

The associate editor coordinating the review of this manuscript and approving it for publication was Chulhong Kim.



FIGURE 1. Carotid disease analysis process based on artificial intelligence segmentation method.

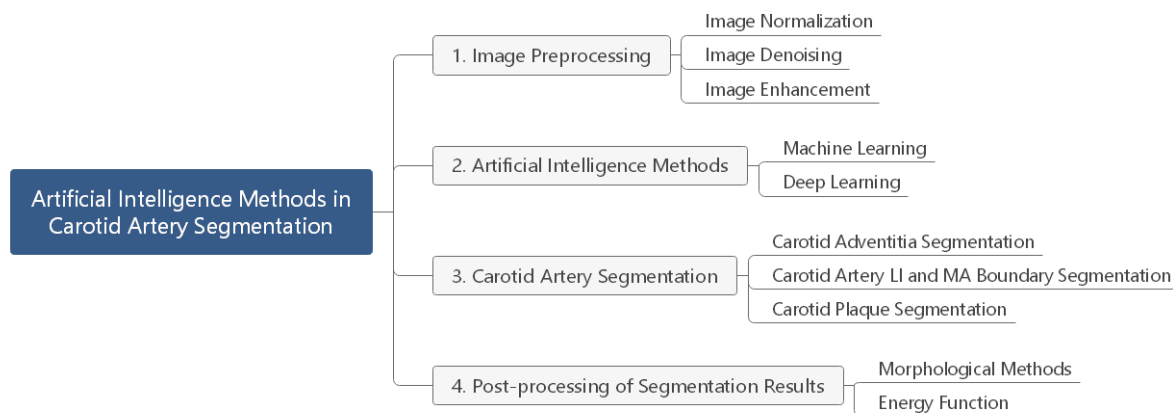


FIGURE 2. Topics in carotid artery segmentation.

area measurement and vulnerability analysis [5]. In order to facilitate doctors to carry out the above measurement and analysis, we need to segment the carotid lumen, media-adventitia (MA), lumen-intima (LI), and plaques to obtain the region of interest (ROI). The carotid artery disease diagnosis process is shown in Figure 1. This paper mainly relates to the second step in Figure 1, Image segmentation. Various technical topics in carotid artery segmentation are shown in Figure 2.

In the early days, carotid artery segmentation mainly applied edge-based [6], region-based [7] and threshold-based [8] methods, but these methods have several limitations [9]. Edge-based segmentation is not effective for images with blurred boundaries; region-based segmentation is prone to over-segmentation, while threshold-based segmentation can not deal with gray-level images with unimodal distribution. In order to address these problems, researchers have used more and more artificial intelligence (AI) methods (traditional machine learning and deep learning) for carotid artery segmentation [10], [11] and achieved many satisfactory results in recent years.

This paper reviews and analyzes the research of traditional machine learning and deep learning in carotid artery segmentation. The remainder of this paper is organized as follows. In Section II, we introduce some public datasets of carotid medical images, the preprocessing methods of medical images. In Section III, we briefly introduce the application of artificial intelligence used in carotid artery segmentation. In Section IV, we present the post-processing methods of the segmentation results. Section V to 7 review and summarize the applications of artificial intelligence in

carotid adventitia, carotid MA and LI boundaries, and carotid plaque segmentation, the segmentation results are shown as Figure 3. Section VIII reviews the current application status, problems, and prospects of artificial intelligence in carotid artery segmentation. Finally, conclusions are given in Section IX.

## II. IMAGE PREPROCESSING

Image preprocessing is of great significance to the segmentation in carotid artery images. Suitable preprocessing methods will positively impact the subsequent feature extraction (whether manual feature extraction in traditional machine learning or high-dimensional feature extraction in deep learning). Faced with different imaging modalities, researchers will use different image preprocessing methods. Due to the physical characteristics of ultrasound, US images usually have low imaging quality, a lot of noise and artifacts, and low contrast between tissues and structures. Therefore, denoising and enhancement are often used in the process of US image preprocessing. Because of their better imaging quality, MR and CT do not need too much preprocessing and often only need to normalize the images. The effects of different traditional preprocessing methods for carotid ultrasound images are shown in Figure 4. In addition to traditional methods, there are many deep learning methods for image processing [15], such as image denoising [16], [17] and image enhancement [18]. These methods can be applied to the preprocessing of carotid artery images. In the rest of this section, we will summarize the public datasets, image normalization, denoising, and enhancement methods of carotid artery image.

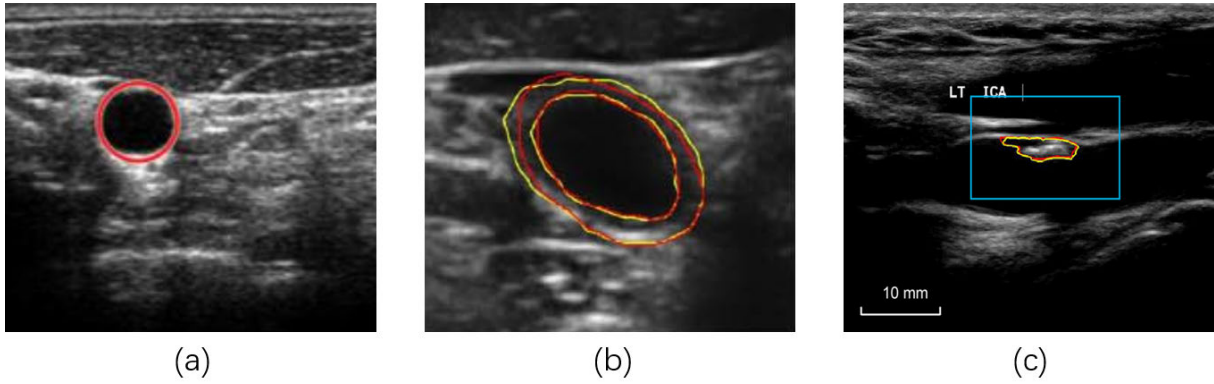


**FIGURE 3.** Segmentation results. (a) The segmentation results of carotid adventitia [12]. (b) The the segmentation results of carotid MA and LI boundaries [13]. The yellow contours show the manual segmentation results and the red contours are the algorithm segmentation results. (c) The the segmentation results of carotid plaque [14]. The yellow contour is the algorithm segmentation results and red contour is the manual segmentation results.

**TABLE 1.** Carotid artery segmentation datasets.

Imaging Modality	Acquire Region	Data size	Data Purpose	Reference
CT	Carotid bifurcation	56	Carotid artery lumen segmentation	[19]
US	Cross-sectional of carotid artery	283	Carotid adventitia segmentation	[20]
US	Carotid bifurcation	80	Carotid plaque segmentation	[21]
US	Coronary artery	435	Carotid lumen and media segmentation	[22]

**A. PUBLIC DATASETS OF CAROTID ARTERY IMAGES**

Compared with the public datasets in other fields, there are few public datasets in the medical field, which is a significant problem faced by the large-scale applications of artificial intelligence in the medical field. We will introduce some public datasets for carotid segmentation in this section.

CLS2009 [19] is a dataset of CTA at the bifurcation of the carotid artery. The dataset consists of 56 CTA datasets from three different medical centers and is used for adventitia segmentation of 3D carotid artery CT images. Artery dataset [20] is a dataset of 283 cross-sectional ultrasound images of the carotid artery for carotid adventitia segmentation. CCA [21] contains B-mode and blood flow longitudinal ultrasound images of the common carotid artery bifurcation and they are used for the segmentation of carotid plaque. IVUS [22] contains 435 intra vascular ultrasound (IVUS) frames (109 train frames and 326 test frames) from 10 patients. Each frame has been manually annotated for the lumen and MA borders by four clinical experts. Table 1 summarize some of the available datasets for carotid artery segmentation.

**B. IMAGE NORMALIZATION**

Image normalization is a process of image feature scaling, which aims to scale the features of different dimensions to the same range, increase the weight of small variance features, and weaken large variance features so that the original

features of different dimensions have the same weight effect on the final result. For example, some studies rely on carotid artery images collected using multiple devices in carotid artery segmentation. The gray values of different images are different, so there are differences between features. Therefore, it is necessary to normalize the images to make the feature weights of different images are the same. There are usually two methods for image normalization. One is to scale the feature to [0, 1], and the other is to scale the feature to [-1, 1]. [23], [24], and [25] used image normalization in their experiments based on the following equations,

$$X_{new} = \frac{X_i - X_{min}}{X_{max} - X_{min}} \tag{1}$$

$$X_{new} = \frac{X_i - X_{mean}}{X_{max} - X_{min}} \tag{2}$$

Eq. 1 and Eq. 2 denote scaling features to [0, 1] and [-1, 1], respectively.  $X_{new}$  represents the normalized pixel value,  $X_i$  represents the original pixel value,  $X_{max}$  and  $X_{min}$  represent maximum and minimum pixel values, and  $X_{mean}$  represents average pixel values.

**C. IMAGE DENOISING**

Noise will be generated in the collection, transmission, and analysis of medical images (especially ultrasonic images). The noise will directly affect the image’s visual effect and affect image feature extraction through an artificial

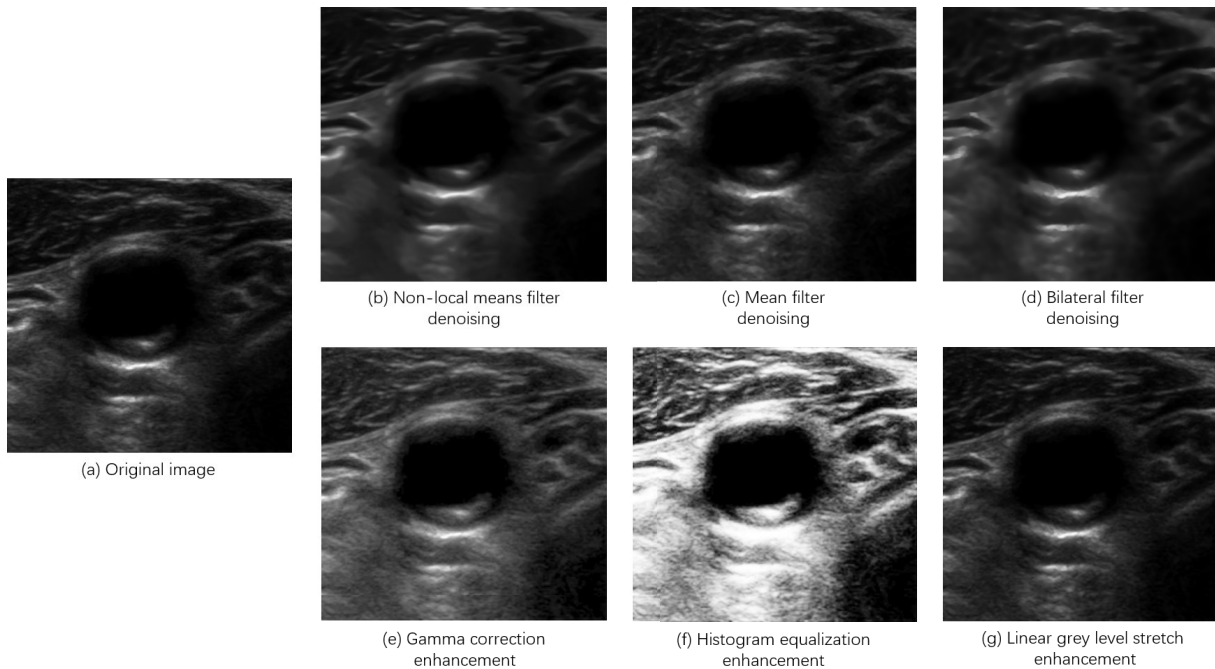


**FIGURE 4.** The effect of carotid image preprocessing methods. (a) Original image, (b) Non-local means filter denoising, (c) Mean filter denoising, (d) Bilateral filter denoising, (e) Gamma correction enhancement, (f) Histogram equalization enhancement, (g) Linear grey level stretch enhancement.

intelligence model. In order to deal with the those problems, we need to denoise the image. Spatial filtering and wavelet filtering are the two most commonly used traditional image denoising methods for image preprocessing. Peak signal-to-noise ratio (PSNR) and structural similarity (SSIM) are usually used to measure image denoising performance.

In carotid image denoising, image denoising is commonly applied to carotid ultrasound images as a preprocessing step prior to inputing images into segmentation models. Researchers mainly use three spatial filtering methods, mean filter [26], non-local means filter [27], and bilateral filter [28]. Mean filter is a convolution operation, which convolves the original image with a mean mask to obtain the denoised image. Mean filter is a method to reduce noise at the expense of image sharpness. Usually, the larger the mask, the better the denoising effect, but the image will become more blurred. Moreover, the convolution operation is a type of neighborhood filtering operation, which only considers the influence of the pixels around on the central pixel but ignores the influence of the global information. Unlike the mean filter, non-local means filter [29] is a global filtering method, which considers the influence of all pixels around the central pixel and can eliminate noise while maintaining the clarity of the image. However, non-local means filter needs to compare each pixel with all other pixels. It takes a lot computation and is time-consuming, and it is not suitable for real-time image denoising. Bilateral filter is also a neighborhood filtering operation, which considers the influence of the spatial distance and gray distance between the center pixel and neighborhood pixels. It can denoise the

image while preserving the boundary. The calculation of center pixel value  $g(i,j)$  of bilateral filter mask is

$$g(i,j) = \frac{\sum_{(k,l) \in S_{k,l}} f(k,l) w_s w_g}{\sum_{(k,l) \in S_{k,l}} w_s w_g} \quad (3)$$

$S_{k,l}$  denotes the neighborhood of  $g(i,j)$ ,  $(k, l)$  is a pixel in  $S_{k,l}$ ,  $f(k,l)$  is the pixel value of  $(k, l)$ .  $w_s$  and  $w_g$  are the spatial distance and gray distance between the center pixel and the neighborhood pixel, respectively.

$$w_s = e^{-\frac{(i-k)^2 + (j-l)^2}{2\sigma_s^2}} \quad (4)$$

$$w_g = e^{-\frac{\|f(i,j) - f(k,l)\|^2}{2\sigma_g^2}} \quad (5)$$

where  $\sigma_x$  is the Gaussian coefficient, and  $f(i,j)$  is the pixel value of the original central pixel.

Wavelet denoising is another method for carotid image denoising, [30] uses curvelet filtering [31], and [32] uses Wiener filtering in wavelet domain. The process of wavelet denoising is to transform the original image based on a variety of basic functions. And then, the transformed signal is processed based on a threshold or combined with spatial filtering.

#### D. IMAGE ENHANCEMENT

Compared with MR and CT images, the imaging quality of US is relatively poor, and the contrast between tissue structures is low. Many studies on ultrasound images need to enhance the image in order to enhance the boundary,



**FIGURE 5.** Gray value curve of linear grey level stretch and Gamma correction.

outline, or contrast of the whole image to improve the readability, which will be convenient for observation and further analysis and processing. Grayscale transformation is the most commonly used image enhancement method in carotid ultrasound images, such as linear grey level stretch [13], [33], histogram equalization [28], and Gamma correction [32].

Linear grey level stretch and Gamma correction are methods to directly transform the grayscale value  $r$  of the input image. Linear grey level stretch changes the gray value function of the input image into a piecewise function, thus changing the contrast of the original image. Gamma correction is the power-law transformation of the original gray value, and the output gray value is set to  $s$ , Gamma correction function is  $s = cr^\gamma$ , where  $c$  and  $\gamma$  are positive numbers. Figure 5 shows the gray value curves of linear grayscale stretching and gamma correction. The histogram equalization is to change the gray value of the unimodal distribution into a uniform distribution, thereby increasing the image's contrast and achieving image enhancement.

### III. ARTIFICIAL INTELLIGENCE METHODS USED IN CAROTID ARTERY SEGMENTATION

The earliest use of AI in healthcare dates back to 1972, when Tim De Domabal and Susan Clamp, two scientists at the University of Leeds in the United Kingdom, developed a system for diagnosing the cause of abdominal pain based on Bayesian models. Subsequently, artificial intelligence methods began to be used frequently in the medical field. Compared to manual diagnosis, AI diagnostic methods are efficient and objective. Traditional machine learning and deep learning are two AI methods, and we will briefly introduce these two methods used for carotid artery segmentation.

#### A. TRADITIONAL MACHINE LEARNING

Machine learning can be understood as the processing and learning of existing data to summarize a specific set of rules and build a predictive model to analyze new data accordingly.

There are two main steps, features extraction and learning. The extraction of data features relies on manual extraction and then on classifiers to complete the features learning. Figure 6 illustrates the workflow of the traditional machine learning for the carotid segmentation task.

In processing medical images, the main focus is on extracting pixel gray value features, texture features, and morphological features. Pixel gray value features do not require special extraction, and, usually, the preprocessed image is passed directly into the feature learning model [34]. Texture features describe the surface features of an image and represent both local features and global features [35]. In carotid segmentation, texture features mainly rely on statistical methods for measurement, such as grayscale co-occurrence matrix [28]. Morphological features refer to the features obtained by extracting the shape or color of the target area. For example, we can extract the edge of the carotid artery in carotid artery segmentation and obtain shape features [30]. When multiple features are obtained, we can fuse or select the features and then input them to a classifier for feature learning.

Learning on features can usually be divided into two main categories, supervised learning and unsupervised learning. Supervised learning refers to the category label that already has the features to be classified. The classifier needs to establish a function to classify the features to make the results consistent with the labels. Unsupervised learning means that the category labels of the features do not exist, and the classifier needs to find some attributes of the features and then classify them. In carotid segmentation, commonly used supervised learning classifiers include Bayesian classifiers [36], [37], support vector machines [34], [38], random forests [32], and their improved versions. Unsupervised learning mainly uses clustering methods [10], [30]. In addition to the above traditional classifiers, some shallow artificial neural networks are also used as classifiers and applied to carotid segmentation [39], [40].

#### B. DEEP LEARNING

Deep learning is currently the most popular artificial intelligence method and has achieved impressive results in various fields. Compared with traditional machine learning, deep learning can avoid the manual extraction of features and, instead, relies on its deep neural network to extract features. At the same time, thanks to the depth of neural networks and the nonlinear operations brought through the activation function, deep learning can simultaneously accomplish low, medium, and high-dimensional feature extraction instead of being limited to the relatively low-dimensional features extracted manually. The extracted features are classified at pixel level to get the category of each pixel, so as to achieve the purpose of image segmentation. At present, many researchers have used deep learning to segment carotid artery images [13], [23], [25], [41]. The workflow of deep learning in the carotid segmentation task is given in Figure 7.

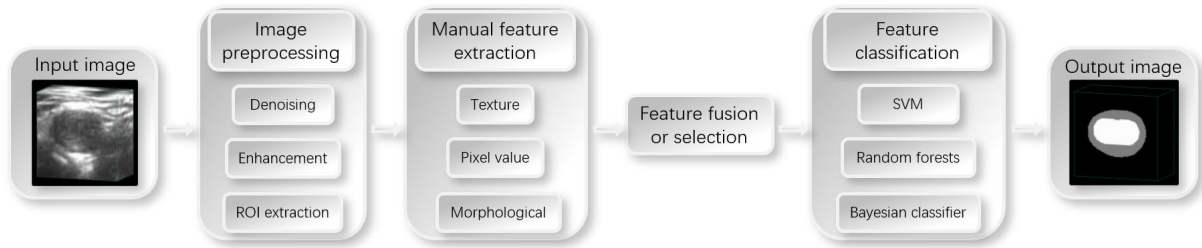


FIGURE 6. Traditional machine learning segmentation process.

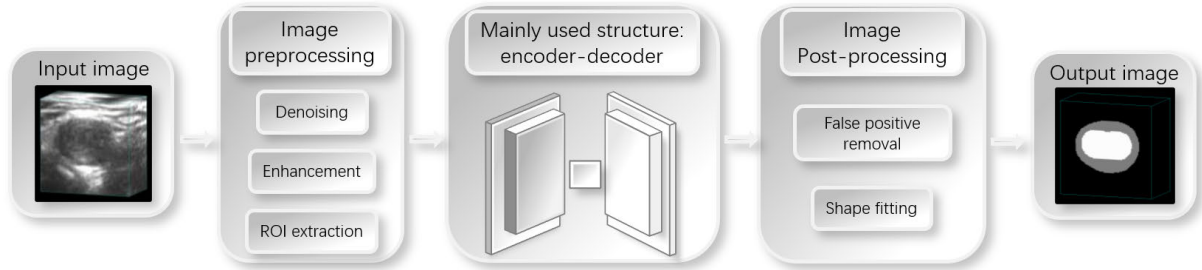


FIGURE 7. Deep learning segmentation process.

The most commonly used deep learning network in the carotid segmentation is the convolutional neural network (CNN) [42], [43], first proposed by LeCun in 1989 [44]. CNN have various network structures, and encoder-decoder structure is the most used CNN structure for carotid segmentation [24], [45], which usually contains convolutional layer, pooling layer, activation function, and upsampling layer. Among them, the convolutional and pooling layers are responsible for extracting multi-dimensional features from input data; The activation function is used to introduce nonlinear transformation into CNN to address the problem of insufficient expression ability of linear convolution operation; The upsampling layer realizes the restoration of the input image and the pixel by pixel classification, that is, segmentation. In carotid artery segmentation, in addition to the network structure of neural network, there are some other designs that can affect the performance of neural network, such as the receptive field and loss function. We will briefly introduce them below.

1) RECEPTIVE FIELD

Receptive field (RF) is the size of the mapped region of the pixel points on the output feature map of CNN on the original image, which can also be understood as the amount of contextual information of the original image contained in the pixel points on the output feature map, as shown in Figure 8. In a carotid plaque segmentation research, the original U-Net was modified to increase RF by using dilated convolution [42]. The RF is calculated as  $RF_i = (RF_{i+1} - 1) \times s_{i+1} + f_{size_i}$ , where  $RF_i$  is the RF size corresponding to the layer  $i$ ,  $s_i$  is the stride of convolution kernel layer  $i$ , and  $f_{size_i}$  is the size of convolution kernel layer  $i$ .

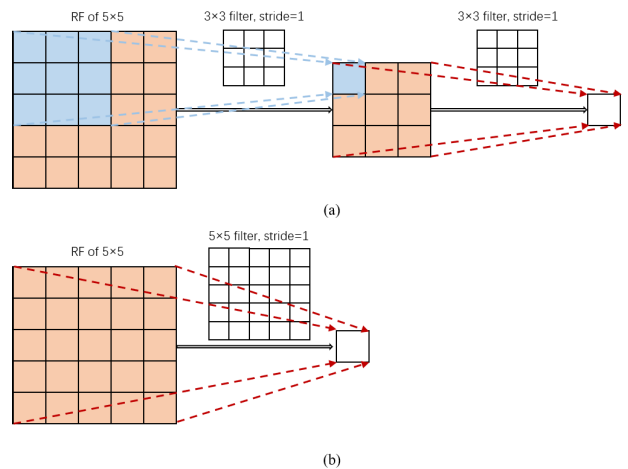


FIGURE 8. (a) RF after two 3 × 3 convolutions is 5 × 5. (b) RF after one 5 × 5 convolutions is 5 × 5.

Figure 8 (a) shows that, after two 3 × 3 convolution operations, the RF corresponding to a pixel point is 5 × 5. Its total number of parameters is  $2 \times c \times (3 \times 3 \times c) = 18c^2$  when the number of channels of both convolution operations is  $c$ . Figure 8 (b) shows that, after a 5 × 5 convolution operation, the RF corresponding to a pixel point is also 5 × 5, and its total number of parameters is  $c \times (5 \times 5 \times c) = 25c^2$  for a channel number of  $c$ . It can be seen that the number of parameters of the small convolution kernel is smaller than large convolution kernel for the same RF, and additional nonlinear operations can be added.

2) LOSS FUNCTION

In deep learning, the image segmentation problem can also be considered as a pixel-by-pixel classification problem, where the pixels belonging to the object are positive samples and

belonging to the background are called negative samples. The category of each pixel is given in the label, and different categories correspond to different values, called true values. The original image is computed by the neural network, which outputs the predicted value for each pixel. The difference between the predicted value and the true value is called the loss. The function that calculates the loss is called the loss function. In image segmentation, the commonly used loss functions are cross-entropy loss and DICE loss.

However, in the carotid segmentation, we will face some unique problems. First, the number of positive samples is much smaller than negative samples. When calculating the loss, the negative samples will account for more loss, making the network focus more on the background than the object. [25] alleviated the problem by combining DICE loss and Focal loss in a carotid segmentation research. Second, the boundary of the carotid artery should usually be smooth and curved, but the predict segmentation result will often have some irregular boundaries. To cope with this problem, [46] designed a new loss function, adding curvature loss, solidity loss, and intersection loss to the original cross-entropy loss, to alleviate the problem of irregular boundary of segmentation results.

#### IV. IMAGE POST-PROCESSING

The boundary of carotid artery is usually smoothly curved, but in some cases, the boundary of carotid artery segmented by artificial intelligence methods can have jagged and irregular shapes. Also, redundant segmentation areas may appear. In this case, we need to use some post-processing methods to improve the segmentation results to match the actual situation of carotid artery.

The opening-and-closing operation is a basic morphological operation that can improve the jaggedness of carotid segmentation boundary. References [23] and [28] used this method in carotid adventitia segmentation and carotid MA and LI boundary segmentation, respectively, to improve the segmentation results. The energy functional model can further improve the curve of the segmentation results to make it closer to the actual boundary of carotid artery and avoid irregular segmentation. References [26] and [12] used an energy functional model in carotid artery segmentation. The main idea of the energy functional model is to create a deformable parameter profile (segmentation result profile) and a corresponding energy function. The energy function represents the gap between the parametric profile and the actual profile. The smaller the gap, the smaller the energy. The energy is minimized by changing the parameters of the parameter curve. When the energy reaches a minimum, the parameter profile is closest to the actual profile.

False-positive region removal is to remove the redundant regions which are not targets in the segmentation results. In carotid segmentation, connected component analysis is the most commonly used method for false-positive region removal. [23], [25], and [47] use this method in post-processing. Through the connected component analysis,

regions that are not connected to the region of interest can be removed.

#### V. CAROTID ADVENTITIA SEGMENTATION

The common carotid artery is the most important artery supplying blood to the head, divided into the left common carotid artery and the right common carotid artery. The two common carotid arteries bifurcate into the neck region's external carotid artery and the internal carotid artery [48]. The common carotid artery is relatively narrow and has a Y-type bifurcation structure, prone to vascular occlusion. Carotid stenosis does not cause any symptoms early, and people do not realize a problem until stroke occurs [12]. Therefore, it is necessary to examine the carotid artery regularly and analyze the degree of carotid artery stenosis. To analyze this information, the carotid artery needs to be identified and depicted from carotid artery images, which is usually done manually by doctors. However, manually identifying and depicting the carotid artery is difficult and time-consuming. Automatic localization and segmentation of carotid adventitia make it convenient for doctors to analyze carotid artery stenosis. Table 2 summarizes some related research in the carotid adventitia segmentation.

##### A. DEEP LEARNING IN CAROTID ADVENTITIA SEGMENTATION

Encoder-decoder networks are one of the most commonly used deep learning segmentation networks, and U-Net [51] and its modified versions are representatives of encoder-decoder networks. Many researchers have segmented the carotid epicardium using U-Net-based networks or self-designed encoder-decoder networks. Azzopardi et al. [50] used an encoder-decoder network, deep convolutional neural network (DCNN), for carotid US image segmentation. First, they applied a phase coherence process to the carotid ultrasound images. This processing avoids the effect of different ultrasound image brightness and provides a feature space that is robust to image brightness variations. Then, the phase-coherent mapping of the original ultrasound images was used as the input of DCNN for carotid segmentation and obtained good segmentation results. Jiang et al. [49] integrated three U-Net and inception structures [52] for carotid artery 3D ultrasound images to segment the carotid adventitia. First, they divided the 3D ultrasound images into 2D images in axial, lateral, and frontal directions. Then inputted them into the three U-Net with non-shared parameters for segmentation to obtain three directions segmentation results. Next, the segmentation results in the lateral and frontal directions were reconstructed into 3D images, and the 2D images in the axial direction were acquired separately. Finally, the three sets of 2D images in the axial direction are combined and input to a segmentation average network based on inception structure to obtain the final output results. The experimental results show that this method outperforms U-Net. Saba et al. [24] used VGG16 [53] as an encoder and fully convolutional networks

TABLE 2. Carotid adventitia segmentation.

Method	Imaging modality	Data size	Model or structure	Preprocessing	Post-processing	Performance	Paper
DL	3D MR	194	Modified DeepMedic	Zero mean and unit variance	False positive removal	DSC: 0.80 ± 0.13	[23]
	3D CT	56	Optimized 3D U-Net	Intensity normalization	False positive removal	DSC: 0.823	[25]
	3D US	23808	Modified U-Net	/	/	DSC: 0.675	[49]
	2D US	2156	U-Net	/	/	DSC: 0.943	[11]
		407	Encoder - decoder	/	/	/	[24]
		500	Encoder - decoder	Phase congruency maps	/	DSC: 0.988	[50]
		283	Faster R-CNN	/	Shape fitting	Jaccard: 0.9086	[12]
		150	Modified U-Net	Non-local means filter	/	DSC: 0.8722	[27]
ML		302	Modified U-Net	/	Fals positive removal	DSC: 0.95	[47]
	2D US	361	Clustering	Curvelet filtering	/	/	[30]

Dice similarity coefficient (DSC), Jaccard similarity coefficient (Jaccard).

(FCN) [54] as a decoder to segment the near wall and far wall of LI with good performance. Pramulen et al. [27], Xie et al. [11], [47], and Zhou et al. [25] segmented the carotid arteries using their modified U-Net, respectively, and all achieved satisfactory results. In a carotid ultrasound image segmentation study, Hassanin et al. [12] proposed a two-step segmentation method. First, the Faster region-based convolutional network (R-CNN) [55] was used for initial detection of the common carotid artery region, and then the localization methods and snake segmentation method were used for detailed segmentation.

**B. MACHINE LEARNING IN CAROTID ADVENTITIA SEGMENTATION**

Although DL methods have received more attention in recent years, traditional ML has also been applied in carotid segmentation studies. For example, in 2021, Latha et al. [30] performed segmentation of carotid ultrasound images using a clustering approach. The image was first denoised using Curvelet filtering, and then edge detection was performed using a modified affinity propagation method. The edge-detected images were input to a density-based spatial clustering method for carotid adventitia segmentation. They compared the clustering method with the gradient vector flow (GVF) snake model and particle swarm optimization (PSO) clustering method and demonstrated the effectiveness of the clustering method. A summary of the related deep learning and machine learning research in carotid adventitia segmentation is given in Table 2.

**VI. CAROTID ARTERY LI AND MA BOUNDARY SEGMENTATION**

Carotid intima-media thickness (CIMT) is an important biological indicator of cardiovascular disease. A study analyzing the risk of cardiovascular disease in 5858 subjects showed that a CIMT > 1.18 mm leads to an increased incidence of stroke [56]. The measurement method of CIMT

is to identify the boundary of LI and MA and then calculate the vertical distance between them. However, LI and MA are difficult to identify and depict manually. Therefore, accurate LI and MA segmentation are of great importance for CIMT measurements. Early segmentation methods mainly use low-dimensional image processing methods, such as edge detection, morphological methods. However, with the emergence of artificial intelligence methods with great potential in medical applications, more and more researchers are applying artificial intelligence methods to medical image segmentation, including carotid LI and MA segmentation. The studies on LI and MA boundary segmentation are summarized in Table 3 and the reviewed as follows.

**A. DEEP LEARNING IN CAROTID ARTERY LI AND MA BOUNDARY SEGMENTATION**

In recent studies of carotid LI and MA boundary segmentation using deep learning methods, U-Net and its improved versions are the most frequently used deep learning models by researchers. Azzopardi et al. [46] used 750 carotid ultrasound images for segmentation of LI and MA boundaries. Since the 750 ultrasound images do not have the same brightness, they first extracted the phase coherence information and then fed the extracted information into a U-Net with a geometrically constrained (GC) loss function for segmentation. Using the GC loss function alleviates the jaggedness problem of the segmented LI and MA boundaries and the problem of intersection of the two boundaries. Jiang et al. [43] conducted a carotid 2D ultrasound image segmentation study in 2021. In this study, they first flipped the original ultrasound images horizontally and vertically. Then the original image, horizontally flipped image, and vertically flipped image were input into three U-Net to obtain three outputs. Next, the segmentation results of the two flipped images are flipped back to the original orientation. Finally, the three segmented images use a pixel-level majority voting strategy to obtain the final LI and MA boundary segmentation results.



**TABLE 3. Carotid artery lumen-intima and media-adventitia segmentation.**

Method	Imaging modality	Data size	Model or structure	Preprocessing	Post-processing	Performance (MA, LI)	Paper
DL	3D MR	27	3D residual U-Net	/	/	/	[41]
	2D MR	12390	CNN	Intensity normalization	/	DSC: 0.9542, 0.9475	[57]
	3D US	1007	FCN	Linear grey level stretch	Continuous max-flow	DSC: 0.973, 0.960	[13]
		144	U-Net	Linear grey level stretch, Adaptive region-based distribution function	/	DSC: 0.9646 ± 0.0222, 0.9284 ± 0.0446	[33]
	2D US	224	Modified U-Net	/	/	DSC: 0.951 ± 0.041, 0.916 ± 0.066	[43]
		220	CNN	Image normalization	/	/	[58]
		326	FCN	/	Ellipse fitting	Jaccard: 0.80, 0.84	[59]
		408	FCN	/	/	/	[60]
		396	Encoder-decoder	/	/	/	[61]
		/	Modified U-Net	Despeckle filter	/	DSC: 0.962 ± 0.34, 0.925 ± 0.49	[46]
ML	2D US	/	Sparse autoencoder	Mean filter	Active contour	XXX	[26]
		240	ANN	/	/	Jaccard: 0.91353, 0.91828	[40]
	67	AE	/	/	/	[62]	
	55	AE	/	/	/	[39]	
	200	Clustering	/	/	/	[10]	
	45	ELM	/	/	/	[63]	
	49	SVM	Bayesian least square estimation filter	/	/	[38]	
	25	ELM	/	/	/	[64]	
	70	Random forest	Wiener filtering in wavelet domain, adaptive gamma correction	/	/	[32]	
	/	Bayesian	/	/	/	[37]	

Artificial neural network (ANN), autoencoder (AE), extreme learning machine (ELM), and support vector machine (SVM), dice similarity coefficient (DSC), Jaccard similarity coefficient (Jaccard).

Zhou et al. [33] used patch-level and pixel-level classification to segment LI and MA, respectively. First, they divided the original image into multiple  $64 \times 64$  patches, classified each patch using a CNN model to determine whether the patch was the MA boundary, and then reorganized the classified patches to obtain the MA boundary. At the same time, they use U-Net to segment the original graph to obtain the boundary of LI. Finally, the two boundaries are combined to derive the final segmentation result. In a study of carotid 3D MR images, the carotid LI and MA boundaries were segmented using 3D residual U-net [41]. The first step was to segment the carotid lumen at patch and global levels on MR images, and two segmentation results were obtained. Next, the segmentation results were integrated to obtain the third set of segmentation results. Finally, the three sets of results were combined with the original MR images and input to the iterative 3D residual U-Net for carotid lumen and wall segmentation. Besides U-Net, FCN is also a common carotid segmentation network used by researchers, such as [13], [57], [59], [60], and [61].

### B. MACHINE LEARNING IN CAROTID ARTERY LI AND MA BOUNDARY SEGMENTATION

Before the great popularity of deep neural networks, machine learning methods using shallow neural networks (such as autoencoder and its modified versions) were often used for carotid LI and MA boundary segmentation. Su et al. [26] conducted a segmentation study of LI and MA boundaries using a sparse autoencoder machine. In MA boundary

segmentation, they first input the original image into a first sparse autoencoder, classify each pixel in the image within and outside the MA boundary, and obtain the rough segmentation result of MA boundary. Then, the result is input into a second sparse autoencoder for secondary pixel-level classification, and the rough segmentation result is improved to obtain the final MA boundary segmentation image. Next, LI boundary segmentation is performed using the same method as above. Finally, the active contour model [69] is used to smooth the LI and MA boundaries. The experimental results show that the method has a high agreement with the manual method. References [39], [40], [63], and [62] also segmented the LI and MA boundary using shallow neural networks. In addition to shallow neural networks, traditional machine learning methods are also used for LI and MA boundary segmentation. Nagaraj et al. [38] conducted a carotid LI and MA boundary segmentation study in 2019. In the experiment, the carotid ROI region was first extracted through morphological gradient and watershed transformation. Then, the features of each pixel point were obtained using radial basis function and, finally, the extracted features were input to support vector machine (SVM) for pixel-level classification to segment the LI and MA boundaries.

### VII. CAROTID PLAQUE SEGMENTATION

Ischemic stroke is the most common type of stroke caused by the rupture of unstable plaques in blood vessels, which forms a thrombus and causes cerebral ischemia. Therefore,

**TABLE 4. Carotid artery plaque segmentation.**

Method	Imaging modality	Data size	Model or structure	Performance	Paper
DL	3D US	26	Modified U-Net	DSC: 0.9072 ± 0.062	[65]
	2D US	500	U-Net	DSC: 0.69	[66]
		8484	DenseNets	/	[67]
		510	U-Net ++	/	[14]
ML	2D US	352	Modified U-Net	DSC: 0.80	[42]
		8988	Bayesian	/	[36]
		29	/	DSC: 0.81 ± 0.041	[34]
		150	Clustering	/	[28]
		300	Clustering	/	[68]

Dice similarity coefficient (DSC).

**TABLE 5. Carotid artery segmentation using 3D images.**

Paper	Segmentation object	Imaging modality	Image processing method
[23]	Carotid adventitia	3D MR	Images are divided in the sagittal plane.
[25]	Carotid adventitia	3D CTA	Images are divided in the axial, sagittal, and coronal planes.
[49]	Carotid adventitia	3D US	Images are divided in axial, lateral and frontal slices.
[13]	LI and MA	3D US	Images are divided in the sagittal plane.
[41]	LI and MA	3D MR	Images are divided in the sagittal plane.
[33]	LI and MA	3D US	Images are divided in the sagittal plane.
[65]	Carotid artery plaque	3D US	Images are divided in the sagittal plane.

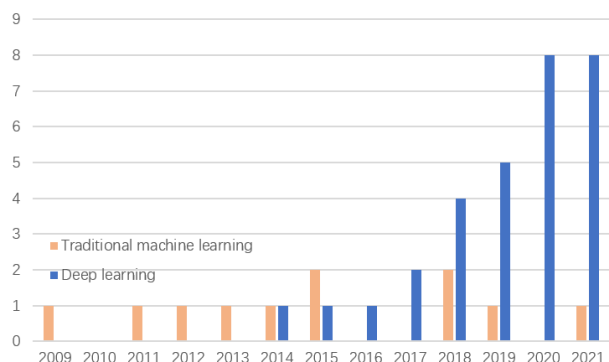


**FIGURE 9. Comparison of the number of papers on carotid artery segmentation using traditional machine learning and deep learning from 2009 to 2021.**

the detection and analysis of atherosclerotic plaques are clinically important for risk level prediction and treatment plan determination for cardiovascular and cerebrovascular diseases. The analysis of atherosclerotic plaques mainly contains plaque surface appearance, plaque density, total plaque area (TPA), and total plaque volume (TPV). Among them, plaque surface appearance is considered one of the crucial factors involved in sudden plaque rupture [70]. TPA and TPV are important indicators to detect the progression and regression of carotid atherosclerosis [71], [72] and are better predictors of first-ever ischemic stroke than the assessment of carotid intima-media thickness [73]. The analysis of various indexes of atherosclerotic plaques is closely related to the accurate identification and segmentation of atherosclerotic plaque. Therefore, many scholars have studied the automatic segmentation of carotid plaques. Table 4 summarizes the research on carotid plaque segmentation.

**A. DEEP LEARNING IN CAROTID PLAQUE SEGMENTATION**

DL network structures commonly used in carotid plaque segmentation studies are also encoder-decoder structures, with U-Net and its modified versions being the most widely used. Xie et al. [66] used three methods to segment carotid plaques. The first method uses the original U-Net to segment the carotid plaque. The second method uses a dual cascade U-Net approach, segmenting the vascular region with the first U-Net and then feeding the vascular region into the second U-Net to segment the plaque. The third method is to segment carotid vessels and plaques simultaneously using dual decoder U-Net. The two decoders correspond to vessel segmentation and carotid plaque segmentation, respectively. The experimental results show that the cascaded U-Net structure has better segmentation performance. Zhou et al. [65] used U-Net to segment carotid plaques. This experiment acquired 294 2D ultrasound images from 34 3D ultrasound images, and only some of the 2D ultrasound images were labeled. They first pre-trained U-Net using unlabeled data. Then the pre-trained U-Net is trained using labeled data to obtain the final segmentation results. They compared this method with the level set method, and the results show that this method achieves better segmentation results. Zhou et al. [14] used carotid ultrasound images to train U-Net++ [45] using eight different backbone networks. The eight output results were then fused using a feature fusion method [74] to obtain the final segmentation results. The segmentation result is better than U-Net.

**B. MACHINE LEARNING IN CAROTID PLAQUE SEGMENTATION**

Traditional machine learning also contributes to the segmentation of carotid plaques. Destremes et al. [36] combined

motion field estimation with a Bayesian model for plaque segmentation of carotid ultrasound videos. The motion field estimation method is first applied to predict the shape and position of the plaque in the current frame of the video and then input to a Bayesian model for detailed plaque segmentation. Qian et al. [34] conducted a study on carotid plaque segmentation. In this study, they first used a superpixel algorithm and Real AdaBoost method [75] to perform region of interest extraction on the original ultrasound images. The extracted ROIs are then fed into a feature classifier based on contextual information for pixel-level classification to obtain segmentation results. In this experiment, the authors used four classifiers, which are SVM with linear kernel [76], SVM with RBF kernel [77], AdaBoost, and random forest [78]. The experimental results show that the method is useful for carotid ultrasound image plaque segmentation and plaque load measurement. Hassan et al. [68] conducted a study on carotid plaque segmentation in 2014. A fuzzy c-means method incorporating spatial information was first used to cluster carotid ultrasound images, and then the results of the clustering were input to a probabilistic neural network classifier for classification to segment carotid plaques.

## VIII. DISCUSSIONS

In the above three sections, we analyse the applications of AI methods in carotid adventitia, LI and MA, and carotid artery plaque, respectively. We find that most of the studies are based on 2D images, but some are based on 3D images. In Table 5, we list the papers that use 3D images for carotid artery research and summarize the processing methods of 3D images.

We have reviewed and discussed in detail the applications of AI in carotid segmentation in the previous sections. The segmentation of carotid image consists of two main steps, feature extraction and feature classification. Researchers use different models to obtain features of various dimensions from images and then feed the extracted features into a classifier for feature classification. Through Figure 9, we can see that more and more researchers are using deep learning for carotid segmentation. The most significant advantage of deep learning over traditional machine learning is the automatic extraction of image features. Deep learning can automatically acquire the image's medium and high dimensional features and then analyze the features. Therefore, the performance of deep learning has greatly exceeded that of traditional machine learning. In addition, we realize that many medical image segmentation studies are based on multi-modality images, such as brain tumor segmentation [79] and cardiac segmentation [80]. However, in the segmentation of carotid artery images, most researchers usually use single-modality images. In future studies, researchers can explore the use of multi-modality images to segment carotid arteries.

In summary, applying AI methods to carotid segmentation has great significance.

1. AI has a fast detection speed, improving the efficiency of carotid artery disease examination.

2. AI relies on the patterns summarized from a large amount of data, which diagnose the disease objectively and assists doctors in decision-making.

3. AI can help doctors who lack experience learn and improve skills and efficiency.

However, AI methods are not without drawbacks. First, AI is a data-driven approach with high requirements on the amount of data. A small number of training data can easily cause overfitting problems, decreasing the generalizability of AI methods. Second, AI has poor interpretability of diagnostic results. Finally, the development of medical AI is inseparable from the close cooperation between medical experts and AI experts. But at present, the cooperation among them is still very limited.

## IX. CONCLUSION

This paper presents a comprehensive review of the applications of AI methods in carotid segmentation. Firstly, the pre-processing methods of carotid medical images and the post-processing methods of segmentation results are discussed. Then, the applications of AI methods in carotid adventitia segmentation, carotid MA and LI boundary segmentation, and carotid plaque segmentation are presented. Finally, the current application status of artificial intelligence methods in carotid segmentation is discussed.

## REFERENCES

- [1] F. Bozkurt, C. Köse, and A. Sari, "An inverse approach for automatic segmentation of carotid and vertebral arteries in CTA," *Expert Syst. Appl.*, vol. 93, pp. 358–375, Mar. 2018.
- [2] L. N. Pu, Z. Zhao, and Y. T. Zhang, "Investigation on cardiovascular risk prediction using genetic information," *IEEE Trans. Inf. Technol. Biomed.*, vol. 16, no. 5, pp. 795–808, Sep. 2012.
- [3] C. P. Loizou, "A review of ultrasound common carotid artery image and video segmentation techniques," *Med. Biol. Eng. Comput.*, vol. 52, no. 12, pp. 1073–1093, 2014.
- [4] P. K. Kumar, T. Araki, J. Rajan, J. R. Laird, A. Nicolaides, and J. S. Suri, "State-of-the-art review on automated lumen and adventitial border delineation and its measurements in carotid ultrasound," *Comput. Methods Programs Biomed.*, vol. 163, pp. 155–168, Sep. 2018.
- [5] M.-H. R. Cardinal, M. H. Heusinkveld, Z. Qin, R. G. Lopata, C. Naim, G. Soulez, and G. Cloutier, "Carotid artery plaque vulnerability assessment using noninvasive ultrasound elastography: Validation with MRI," *Amer. J. Roentgenol.*, vol. 209, no. 1, pp. 142–151, 2017.
- [6] F. Fata, V. Gemignani, E. Bianchini, C. Giannarelli, L. Ghiadoni, and M. Demi, "Real-time measurement system for evaluation of the carotid intima-media thickness with a robust edge operator," *J. Ultrasound Med.*, vol. 27, no. 9, pp. 1353–1361, Sep. 2008.
- [7] F. Molinari, G. Zeng, and J. S. Suri, "Intima-media thickness: Setting a standard for a completely automated method of ultrasound measurement," *IEEE Trans. Ultrason., Ferroelectr., Freq. Control*, vol. 57, no. 5, pp. 1112–1124, May 2010.
- [8] D. J. Williams and M. Shah, "A fast algorithm for active contours and curvature estimation," *CVGIP, Image Understand.*, vol. 55, no. 1, pp. 14–26, 1992.
- [9] M. Jena, S. P. Mishra, and D. Mishra, "A survey on applications of machine learning techniques for medical image segmentation," *Internationa J. Eng. Technol.*, vol. 10, pp. 4489–4495, Nov. 2018.
- [10] J. Alam, M. Hassan, A. Khan, and A. Chaudhry, "Robust fuzzy RBF network based image segmentation and intelligent decision making system for carotid artery ultrasound images," *Neurocomputing*, vol. 151, pp. 745–755, Mar. 2015.
- [11] M. Xie, Y. Li, Y. Xue, L. Huntress, W. Beckerman, S. Rahimi, J. Ady, and U. Roshan, "Vessel lumen segmentation in carotid artery ultrasounds with the U-Net convolutional neural network," in *Proc. IEEE Int. Conf. Bioinf. Biomed. (BIBM)*, Dec. 2020, pp. 2680–2684.

- [12] D. Hassanine, M. Abdellah, A. Khalaf, and R. R. Gharrieh, "Automatic localization of common carotid artery in ultrasound images using deep learning," *J. Adv. Eng. Trends*, vol. 40, no. 2, pp. 127–135, Jul. 2021.
- [13] R. Zhou, F. Guo, M. R. Azarpazhooh, J. D. Spence, E. Ukwatta, M. Ding, and A. Fenster, "A voxel-based fully convolution network and continuous max-flow for carotid vessel-wall-volume segmentation from 3D ultrasound images," *IEEE Trans. Med. Imag.*, vol. 39, no. 9, pp. 2844–2855, Sep. 2020.
- [14] R. Zhou, F. Guo, M. R. Azarpazhooh, S. Hashemi, X. Cheng, J. D. Spence, M. Ding, and A. Fenster, "Deep learning-based measurement of total plaque area in B-mode ultrasound images," *IEEE J. Biomed. Health Informat.*, vol. 25, no. 8, pp. 2967–2977, Aug. 2021.
- [15] Y. Wang, X. Ge, H. Ma, S. Qi, G. Zhang, and Y. Yao, "Deep learning in medical ultrasound image analysis: A review," *IEEE Access*, vol. 9, pp. 54310–54324, 2021.
- [16] H. Wu, R. Wang, G. Zhao, H. Xiao, J. Liang, D. Wang, X. Tian, L. Cheng, and X. Zhang, "Deep-learning denoising computational ghost imaging," *Opt. Lasers Eng.*, vol. 134, Nov. 2020, Art. no. 106183. [Online]. Available: <http://www.sciencedirect.com/science/article/pii/S0143816620301809>
- [17] M. P. Heinrich, M. Stille, and T. M. Buzug, "Residual U-Net convolutional neural network architecture for low-dose CT denoising," *Current Directions Biomed. Eng.*, vol. 4, no. 1, pp. 297–300, Sep. 2018. [Online]. Available: <https://www.degruyter.com/view/journals/cdbme/4/1/article-p297.xml>
- [18] C. Ledig, L. Theis, F. Huszar, J. Caballero, A. Cunningham, A. Acosta, A. Aitken, A. Tejani, J. Totz, Z. Wang, and W. Shi, "Photo-realistic single image super-resolution using a generative adversarial network," in *Proc. IEEE Conf. Comput. Vis. Pattern Recognit. (CVPR)*, Jul. 2017, pp. 4681–4690.
- [19] K. Hameeteman et al., "Evaluation framework for carotid bifurcation lumen segmentation and stenosis grading," *Med. Image Anal.*, vol. 15, no. 4, pp. 477–488, 2011.
- [20] K. Řiha, J. Mašek, R. Burget, R. Beneš, and E. Závodná, "Novel method for localization of common carotid artery transverse section in ultrasound images using modified Viola-Jones detector," *Ultrasound Med. Biol.*, vol. 39, no. 10, pp. 1887–1902, Oct. 2013.
- [21] C. P. Loizou, C. S. Pattichis, M. Pantziaris, and A. Nicolaides, "An integrated system for the segmentation of atherosclerotic carotid plaque," *IEEE Trans. Inf. Technol. Biomed.*, vol. 11, no. 6, pp. 661–667, Nov. 2007.
- [22] S. Balocco et al., "Standardized evaluation methodology and reference database for evaluating IVUS image segmentation," *Computerized Med. Imag. Graph.*, vol. 38, no. 2, pp. 70–90, 2014.
- [23] M. Ziegler, J. Alfraeus, M. Bustamante, E. Good, J. Engvall, E. de Muinck, and P. Dyverfeldt, "Automated segmentation of the individual branches of the carotid arteries in contrast-enhanced MR angiography using DeepMedic," *BMC Med. Imag.*, vol. 21, no. 1, pp. 1–10, Dec. 2021.
- [24] L. Saba, M. Biswas, H. S. Suri, K. Viskovic, J. R. Laird, E. Cuadrado-Godia, A. Nicolaides, N. Khanna, V. Viswanathan, and J. S. Suri, "Ultrasound-based carotid stenosis measurement and risk stratification in diabetic cohort: A deep learning paradigm," *Cardiovascular Diagnosis Therapy*, vol. 9, no. 5, p. 439, 2019.
- [25] T. Zhou, T. Tan, X. Pan, H. Tang, and J. Li, "Fully automatic deep learning trained on limited data for carotid artery segmentation from large image volumes," *Quant. Imag. Med. Surg.*, vol. 11, no. 1, p. 67, 2021.
- [26] S. Su, Z. Hu, Q. Lin, W. K. Hau, Z. Gao, and H. Zhang, "An artificial neural network method for lumen and media-adventitia border detection in IVUS," *Comput. Med. Imag. Graph.*, vol. 57, pp. 29–39, Apr. 2017.
- [27] A. S. Pramulen, E. M. Yuniarno, J. Nugroho, I. M. G. Sunarya, and I. K. E. Purnama, "Carotid artery segmentation on ultrasound image using deep learning based on non-local means-based speckle filtering," in *Proc. Int. Conf. Comput. Eng., Netw., Intell. Multimedia (CENIM)*, Nov. 2020, pp. 360–365.
- [28] M. Hassan, A. Chaudhry, A. Khan, and J. Y. Kim, "Carotid artery image segmentation using modified spatial fuzzy c-means and ensemble clustering," *Comput. Methods Programs Biomed.*, vol. 108, no. 3, pp. 1261–1276, Dec. 2012.
- [29] A. Buades, B. Coll, and J.-M. Morel, "A review of image denoising algorithms, with a new one," *Multiscale Model. Simul.*, vol. 4, no. 2, pp. 490–530, 2005.
- [30] S. Latha, D. Samiappan, P. Muthu, and R. Kumar, "Fully automated integrated segmentation of carotid artery ultrasound images using DBSCAN and affinity propagation," *J. Med. Biol. Eng.*, vol. 41, pp. 1–12, Apr. 2021.
- [31] S. K. Panigrahi, S. Gupta, and P. K. Sahu, "Curvelet-based multiscale denoising using non-local means & guided image filter," *IET Image Process.*, vol. 12, no. 6, pp. 909–918, Jun. 2018.
- [32] H. S. Teja and A. V. Narasimhadhan, "Carotid wall segmentation in longitudinal ultrasound images using structured random forest," *Comput. Electr. Eng.*, vol. 69, pp. 753–767, Jul. 2018.
- [33] R. Zhou, A. Fenster, Y. Xia, J. D. Spence, and M. Ding, "Deep learning-based carotid media-adventitia and lumen-intima boundary segmentation from three-dimensional ultrasound images," *Med. Phys.*, vol. 46, no. 7, pp. 3180–3193, May 2019.
- [34] C. Qian and X. Yang, "An integrated method for atherosclerotic carotid plaque segmentation in ultrasound image," *Comput. Methods Programs Biomed.*, vol. 153, pp. 19–32, Jan. 2018.
- [35] S. Krüg, *Computer Vision Metrics: Survey, Taxonomy, and Analysis*. Cham, Switzerland: Springer, 2014.
- [36] F. Destrempes, J. Meunier, M.-F. Giroux, G. Soulez, and G. Cloutier, "Segmentation of plaques in sequences of ultrasonic B-mode images of carotid arteries based on motion estimation and a Bayesian model," *IEEE Trans. Biomed. Eng.*, vol. 58, no. 8, pp. 2202–2211, Aug. 2011.
- [37] F. Destrempes, J. Meunier, M.-F. Giroux, G. Soulez, and G. Cloutier, "Segmentation in ultrasonic B-mode images of healthy carotid arteries using mixtures of Nakagami distributions and stochastic optimization," *IEEE Trans. Med. Imag.*, vol. 28, no. 2, pp. 215–229, Feb. 2009.
- [38] Y. Nagaraj, A. H. S. Teja, and A. V. Narasimhadhan, "Automatic segmentation of intima media complex in carotid ultrasound images using support vector machine," *Arabian J. Sci. Eng.*, vol. 44, no. 4, pp. 3489–3496, Apr. 2019.
- [39] R.-M. Menchón-Lara and J.-L. Sancho-Gómez, "Fully automatic segmentation of ultrasound common carotid artery images based on machine learning," *Neurocomputing*, vol. 151, pp. 161–167, Mar. 2015.
- [40] R.-M. Menchón-Lara, M.-C. Bastida-Jumilla, J. Morales-Sánchez, and J.-L. Sancho-Gómez, "Automatic detection of the intima-media thickness in ultrasound images of the common carotid artery using neural networks," *Med. Biol. Eng. Comput.*, vol. 52, no. 2, pp. 169–181, Feb. 2014.
- [41] C. Zhu, X. Wang, Z. Teng, S. Chen, X. Huang, M. Xia, L. Mao, and C. Bai, "Cascaded residual U-Net for fully automatic segmentation of 3D carotid artery in high-resolution multi-contrast MR images," *Phys. Med. Biol.*, vol. 66, no. 4, Feb. 2021, Art. no. 045033.
- [42] N. H. Meshram, C. C. Mitchell, S. Wilbrand, R. J. Dempsey, and T. Varghese, "Deep learning for carotid plaque segmentation using a dilated U-Net architecture," *Ultrason. Imag.*, vol. 42, nos. 4–5, pp. 221–230, Jul. 2020.
- [43] M. Jiang, Y. Zhao, and B. Chiu, "Segmentation of common and internal carotid arteries from 3D ultrasound images using adaptive triple U-Net," 2021, *arXiv:2101.11252*.
- [44] Y. LeCun, B. Boser, J. S. Denker, D. Henderson, R. E. Howard, W. Hubbard, and D. L. Jackel, "Backpropagation applied to handwritten zip code recognition," *Neural Comput.*, vol. 1, no. 4, pp. 541–551, 1989.
- [45] Z. Zhou, M. M. R. Siddiquee, N. Tajbakhsh, and J. Liang, "UNet++: Redesigning skip connections to exploit multiscale features in image segmentation," *IEEE Trans. Med. Imag.*, vol. 39, no. 6, pp. 1856–1867, Jun. 2020.
- [46] C. Azzopardi, K. P. Camilleri, and Y. A. Hicks, "Bimodal automated carotid ultrasound segmentation using geometrically constrained deep neural networks," *IEEE J. Biomed. Health Informat.*, vol. 24, no. 4, pp. 1004–1015, Apr. 2020.
- [47] M. Xie, Y. Li, Y. Xue, R. Shafritz, S. A. Rahimi, J. W. Ady, and U. W. Roshan, "Vessel lumen segmentation in internal carotid artery ultrasound with deep convolutional neural networks," in *Proc. IEEE Int. Conf. Bioinf. Biomed. (BIBM)*, Nov. 2019, pp. 2393–2398.
- [48] A. Manbachi, Y. Hoi, B. A. Wasserman, E. G. Lakatta, and D. A. Steinman, "On the shape of the common carotid artery with implications for blood velocity profiles," *Physiolog. Meas.*, vol. 32, no. 12, p. 1885, 2011.
- [49] M. Jiang, J. David Spence, and B. Chiu, "Segmentation of carotid vessel wall using U-Net and segmentation average network," 2020, *arXiv:2002.11467*.
- [50] C. Azzopardi, Y. A. Hicks, and K. P. Camilleri, "Automatic carotid ultrasound segmentation using deep convolutional neural networks and phase congruency maps," in *Proc. IEEE 14th Int. Symp. Biomed. Imag.*, Apr. 2017, pp. 624–628.

- [51] O. Ronneberger, P. Fischer, and T. Brox, "U-Net: Convolutional networks for biomedical image segmentation," in *Proc. Int. Conf. Med. Image Comput. Comput.-Assist. Intervent.* Cham, Switzerland: Springer, 2015, pp. 234–241.
- [52] C. Szegedy, W. Liu, Y. Jia, P. Sermanet, S. Reed, D. Anguelov, D. Erhan, V. Vanhoucke, and A. Rabinovich, "Going deeper with convolutions," in *Proc. IEEE Conf. Comput. Vis. Pattern Recognit. (CVPR)*, Jun. 2015, pp. 1–9.
- [53] K. Simonyan and A. Zisserman, "Very deep convolutional networks for large-scale image recognition," 2014, *arXiv:1409.1556*.
- [54] J. Long, E. Shelhamer, and T. Darrell, "Fully convolutional networks for semantic segmentation," in *Proc. IEEE Conf. Comput. Vis. Pattern Recognit. (CVPR)*, Jun. 2015, pp. 3431–3440.
- [55] S. Ren, K. He, R. Girshick, and J. Sun, "Faster R-CNN: Towards real-time object detection with region proposal networks," *IEEE Trans. Pattern Anal. Mach. Intell.*, vol. 39, no. 6, pp. 1137–1149, Jun. 2017.
- [56] D. H. O'Leary, J. F. Polak, R. A. Kronmal, T. A. Manolio, G. L. Burke, and S. K. Wolfson, "Carotid-artery intima and media thickness as a risk factor for myocardial infarction and stroke in older adults," *New England J. Med.*, vol. 340, no. 1, pp. 14–22, Jan. 1999.
- [57] J. Wu, J. Xin, X. Yang, J. Sun, D. Xu, N. Zheng, and C. Yuan, "Deep morphology aided diagnosis network for segmentation of carotid artery vessel wall and diagnosis of carotid atherosclerosis on black-blood vessel wall MRI," *Med. Phys.*, vol. 46, no. 12, pp. 5544–5561, 2019.
- [58] N. Madian, "Convolutional neural network for segmentation and measurement of intima media thickness," *J. Med. Syst.*, vol. 42, no. 8, pp. 1–8, Aug. 2018.
- [59] J. Yang, L. Tong, M. Faraji, and A. Basu, "IVUS-Net: An intravascular ultrasound segmentation network," in *Proc. Int. Conf. Smart Multimedia*. Cham, Switzerland: Springer, 2018, pp. 367–377.
- [60] M. Biswas, L. Saba, S. Chakraborty, N. N. Khanna, H. Song, H. S. Suri, P. P. Sfikakis, S. Mavrogeni, K. Viskovic, J. R. Laird, E. Cuadrado-Godia, A. Nicolaides, A. Sharma, V. Viswanathan, A. Protogerou, G. Kitas, G. Pareek, M. Miner, and J. S. Suri, "Two-stage artificial intelligence model for jointly measurement of atherosclerotic wall thickness and plaque burden in carotid ultrasound: A screening tool for cardiovascular/stroke risk assessment," *Comput. Biol. Med.*, vol. 123, Aug. 2020, Art. no. 103847.
- [61] M. Biswas, V. Kuppili, T. Araki, D. R. Edla, E. C. Godia, L. Saba, H. S. Suri, T. Omerzu, J. R. Laird, N. N. Khanna, A. Nicolaides, and J. S. Suri, "Deep learning strategy for accurate carotid intima-media thickness measurement: An ultrasound study on Japanese diabetic cohort," *Comput. Biol. Med.*, vol. 98, pp. 100–117, Jul. 2018.
- [62] R.-M. Menchón-Lara, J.-L. Sancho-Gómez, and A. Bueno-Crespo, "Early-stage atherosclerosis detection using deep learning over carotid ultrasound images," *Appl. Soft Comput.*, vol. 49, pp. 616–628, Dec. 2016.
- [63] R.-M. Menchón-Lara, J.-L. Sancho-Gómez, A. Sánchez-Morales, Á. Legaz-Aparicio, J. Morales-Sánchez, R. Verdú-Monedero, and J. Larrey-Ruiz, "Using machine learning techniques for the automatic detection of arterial wall layers in carotid ultrasounds," in *Ambient Intelligence—Software and Applications*. Cham, Switzerland: Springer, 2015, pp. 193–201.
- [64] R.-M. Menchón-Lara, M.-C. Bastida-Jumilla, J. Larrey-Ruiz, R. Verdú-Monedero, J. Morales-Sánchez, and J.-L. Sancho-Gómez, "Measurement of carotid intima-media thickness in ultrasound images by means of an automatic segmentation process based on machine learning," in *Proc. Eurocon*, Jul. 2013, pp. 2086–2093.
- [65] R. Zhou, W. Ma, A. Fenster, and M. Ding, "U-Net based automatic carotid plaque segmentation from 3D ultrasound images," *Proc. SPIE*, vol. 10950, Mar. 2019, Art. no. 109504F.
- [66] M. Xie, Y. Li, Y. Xue, L. Huntress, W. Beckerman, S. A. Rahimi, J. W. Ady, and U. W. Roshan, "Two-stage and dual-decoder convolutional U-Net ensembles for reliable vessel and plaque segmentation in carotid ultrasound images," in *Proc. 19th IEEE Int. Conf. Mach. Learn. Appl. (ICMLA)*, Dec. 2020, pp. 1376–1381.
- [67] M. D. M. Vila, B. Remeseiro, M. Grau, R. Elosua, À. Betriu, E. Fernandez-Giraldez, and L. Igual, "Semantic segmentation with DenseNets for carotid artery ultrasound plaque segmentation and CIMT estimation," *Artif. Intell. Med.*, vol. 103, Mar. 2020, Art. no. 101784.
- [68] M. Hassan, A. Chaudhry, A. Khan, and M. A. Iftikhar, "Robust information gain based fuzzy c-means clustering and classification of carotid artery ultrasound images," *Comput. Methods Programs Biomed.*, vol. 113, no. 2, pp. 593–609, Feb. 2014.
- [69] M. Kass, A. Witkin, and D. Terzopoulos, "Snakes: Active contour models," *Int. J. Comput. Vis.*, vol. 1, no. 4, pp. 321–331, 1988.
- [70] R. U. Acharya, O. Faust, A. P. C. Alvin, S. V. Sree, F. Molinari, L. Saba, A. Nicolaides, and J. S. Suri, "Symptomatic vs. asymptomatic plaque classification in carotid ultrasound," *J. Med. Syst.*, vol. 36, no. 3, pp. 1861–1871, Jun. 2012.
- [71] A. Landry, J. D. Spence, and A. Fenster, "Measurement of carotid plaque volume by 3-dimensional ultrasound," *Stroke*, vol. 35, no. 4, pp. 864–869, 2004.
- [72] J. D. Spence, M. Eliasziw, M. DiCicco, D. G. Hackam, R. Galil, and T. Lohmann, "Carotid plaque area: A tool for targeting and evaluating vascular preventive therapy," *Stroke*, vol. 33, no. 12, pp. 2916–2922, Dec. 2002.
- [73] M. Romanens, "Carotid plaque area and intima-media thickness in prediction of first-ever ischemic stroke: A 10-year follow-up of 6584 men and women: The Tromsø study," *Stroke*, vol. 42, no. 8, pp. 972–978, Aug. 2011.
- [74] J. Yuan, J. Shi, and X.-C. Tai, "A convex and exact approach to discrete constrained TV-L1 image approximation," *East Asian J. Appl. Math.*, vol. 1, no. 2, pp. 172–186, May 2011.
- [75] Y. Freund and R. E. Schapire, "A decision-theoretic generalization of on-line learning and an application to boosting," *J. Comput. Syst. Sci.*, vol. 55, pp. 119–139, Aug. 1995.
- [76] C.-W. Hsu and C.-J. Lin, "A comparison of methods for multiclass support vector machines," *IEEE Trans. Neural Netw.*, vol. 13, no. 2, pp. 415–425, Mar. 2001.
- [77] R. Gilad-Bachrach, A. Navot, and N. Tishby, "Margin based feature selection-theory and algorithms," in *Proc. 21st Int. Conf. Mach. Learn.*, 2004, p. 43.
- [78] L. Breiman, "Random forests," *Mach. Learn.*, vol. 45, no. 1, pp. 5–32, 2001.
- [79] R. Ranjbarzadeh, A. B. Kasgari, S. J. Ghouschi, S. Anari, M. Naseri, and M. Bendechache, "Brain tumor segmentation based on deep learning and an attention mechanism using MRI multi-modalities brain images," *Sci. Rep.*, vol. 11, no. 1, pp. 1–17, May 2021.
- [80] X. Zhuang and J. Shen, "Multi-scale patch and multi-modality atlases for whole heart segmentation of MRI," *Med. Image Anal.*, vol. 31, pp. 77–87, Jul. 2016.

**YU WANG** is currently pursuing the Ph.D. degree with the College of Medicine and Biological Information Engineering, Northeastern University, China. His research interests include deep learning and medical imaging processing.

**YUDONG YAO** (Fellow, IEEE) is currently a Professor with the Department of Electrical and Computer Engineering, Stevens Institute of Technology, USA. His research interests include deep learning and medical imaging processing. He is also a fellow of American Institute for Medical and Biological Engineering (AIMBE).

• • •